

## Charge ordering in the layered Co-based perovskite $\text{HoBaCo}_2\text{O}_5$

E. Suard

*Institute Laue Langevin, 6 Rue Jules Horowitz, BP 156X, 38042 Grenoble Cedex 9, France*

F. Fauth

*Swiss Light Source, Paul Scherrer Institut, 5232 Villigen PSI, Switzerland*

V. Caignaert

*Laboratoire CRISMAT/ISMRA, Boulevard du Marechal Juin, 14050 Caen Cedex, France*

I. Mirebeau

*Laboratoire Léon Brillouin, CE Saclay, 91191 Gif-sur-Yvette, France*

G. Baldinozzi

*Laboratoire SPMS, CNRS-Ecole Centrale de Paris, 92295 Châtenay-Malabry Cedex, France*

(Received 24 February 2000)

From neutron powder diffraction studies performed on the ordered oxygen deficient perovskite  $\text{HoBaCo}_2\text{O}_5$ , we have observed two structural phase transitions at  $T_N \sim 340$  K and  $T_{CO} \sim 210$  K, corresponding to the occurrence of magnetism and the onset of charge ordering, respectively. The charge ordered phase exhibits chains of  $\text{Co}^{2+}$  and  $\text{Co}^{3+}$  along the  $a$  axis and an alternate stacking of these ions along the  $b$  and  $c$  axes. The observed magnetic moments,  $\mu_{\text{Co}^{3+}} = 3.7\mu_B$  and  $\mu_{\text{Co}^{2+}} = 2.7\mu_B$ , confirm this charge ordering and are in good agreement with the expected values for high-spin Co ions in pyramidal environment.

During the last few years, there have been a large number of research activities on the Mn oxides of general formula  $A_{1-x}A'_x\text{MnO}_3$  ( $A$  is a trivalent lanthanide,  $A'$  a divalent alkaline ion) in order to explain the mechanism leading to the colossal magnetoresistivity (CMR) observed in these materials. Up to now, CMR effects have been almost only observed in manganites, although some cobaltates of type  $\text{La}_{1-x}\text{Sr}_x\text{CoO}_3$  also present similar properties, but with far much smaller MR ratios.<sup>1</sup> Recently, however, the highest MR ratios ever observed in Co based oxides have been reported in the perovskite based compounds  $\text{LnBaCo}_2\text{O}_{5.4}$  ( $\text{Ln} = \text{Eu, Gd}$ ).<sup>2</sup> These systems, of general description  $\text{LnBaCo}_2\text{O}_{5+\delta}$  ( $\text{Ln} = \text{trivalent lanthanide}$ ,  $0 \leq \delta \leq 1$ ), appear very interesting since they display a large variety of magnetic and transport properties depending on the oxygen concentration.<sup>3-6</sup> Similarly to what was observed in the manganites, it is likely that the magnetic and transport properties in  $\text{LnBaCo}_2\text{O}_{5+\delta}$  are driven by the mixed valence state of the cobalt ions, expressed by the relations  $\text{Co}^{2+}:\text{Co}^{3+} = (1/2-\delta):(1/2+\delta)$  for  $\delta \leq 0.5$  and  $\text{Co}^{4+}:\text{Co}^{3+} = (\delta-1/2):(3/2-\delta)$  for  $0.5 \leq \delta$ . When increasing  $\delta$  in the generic system  $\text{LnBaCo}_2\text{O}_{5+\delta}$ , the extra oxygen ions are expected to fill the  $\text{Ho}\square$  layer, thus providing an octahedral environment for some of the Co ions. At the limit  $\delta = 1$ , all Co ions are in an octahedral environment and for the particular compound  $\text{LaBaCo}_2\text{O}_6$ , the structure was found to be cubic or orthorhombic.<sup>3,7</sup> Furthermore, in the nonstoichiometric cases ( $\delta \neq 0, 1$ ), complex crystal structures have been postulated in order to localize the extra oxygen ions.<sup>5,8</sup> These assumed crystal structures lead to mixed octahedral and pyramidal environments for the Co ions, with nonnegligible consequences on their electronic structure. Up to now, only

the crystal structures of both the stoichiometric case  $\text{LaBaCo}_2\text{O}_6$  (Ref. 7) and the oxygen deficient case  $\text{HoBaCo}_2\text{O}_5$  (subject of the present study) have been precisely determined by means of neutron powder diffraction. In these particular compounds, the cobalt environment appears to be either exclusively octahedral ( $\delta = 1$ ) or pyramidal ( $\delta = 0$ ). Therefore, it is clear that the  $\text{LnBaCo}_2\text{O}_{5+\delta}$  system is able to reproduce a large set of Co ion configurations. When further considering that trivalent and/or tetravalent cobalt ions are known to display multiple electronic structures, these compounds deserve a careful study in the future to assess the magnetic properties of  $\text{Co}^{2+}$ ,  $\text{Co}^{3+}$ , and  $\text{Co}^{4+}$  ions as a function of their relative ratios and local environment.

In this paper, we report the temperature dependent study of the pure oxygen deficient cobaltate  $\text{HoBaCo}_2\text{O}_5$ . Since the  $\text{Co}^{2+}:\text{Co}^{3+}$  ratio is exactly one in this compound, we anticipate charge ordering (CO) to occur, that is a real-space ordering of divalent and trivalent cobalt ions. Similar effects have been frequently reported in the manganites  $A_{1/2}A'_{1/2}\text{MnO}_3$ , but in almost all these cases, the CO state was accompanied by the onset of an antiferromagnetic phase at a Néel temperature  $T_N \leq T_{CO}$ .<sup>9</sup> In a few cases, the change in crystal symmetry induced by charge ordering could be directly observed, generally by using synchrotron<sup>10</sup> and/or electron diffraction techniques.<sup>11</sup> In  $\text{HoBaCo}_2\text{O}_5$ , we observe by means of neutron powder diffraction, the onset of a CO phase below  $T_{CO} \sim 210$  K. The charge ordering is reflected by the doubling of the crystallographic unit cell along the  $b$  direction and a change in the space-group symmetry (space group  $Pmmb$ ). This transition is coupled to an increase of the insulating behavior of  $\text{HoBaCo}_2\text{O}_5$ . More interestingly, this

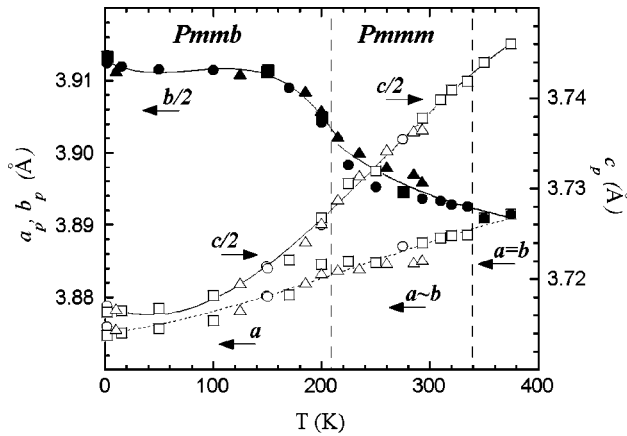


FIG. 1. Temperature dependence of the pseudocubic cell parameters in  $\text{HoBaCo}_2\text{O}_5$ .

CO transition, which is accompanied by a considerable jump in the resistivity, occurs far below the paramagnetic to antiferromagnetic transition at  $T_N \sim 340$  K, where a first increase in the resistivity curve is already observed.

The  $\text{HoBaCo}_2\text{O}_5$  sample was synthesized using a two-step method which was already successfully applied to produce the related compound  $\text{LaBaMn}_2\text{O}_5$ .<sup>12</sup> The oxygen stoichiometry of our compound is determined to be  $5 \pm 0.01$  from neutron powder diffraction (NPD) experiments. High-resolution NPD measurements were performed at selected temperatures ranging from 1.5 K to 375 K on the instruments D1A ( $\lambda = 1.911$  Å) and D2B ( $\lambda = 1.594$  Å,  $\lambda = 1.05$  Å) at the Institute Laue-Langevin. Due to the weakness of the CO induced superstructure peaks, additional NPD measurements were performed on  $\text{HoBaCo}_2\text{O}_5$  on the high intensity diffractometer G6-1 ( $\lambda = 4.75$  Å) at the Laboratoire Léon Brillouin, which provides powder patterns of remarkably high signal to background ratio. NPD data were refined by the Rietveld method using the program FULLPROF.<sup>13</sup> Electron-diffraction experiments, differential scanning calorimetry (DSC), and resistivity measurements were performed on  $\text{HoBaCo}_2\text{O}_5$  using standard procedures whose descriptions are beyond the scope of this paper. The precise synthesis method, as well as the detailed study of the magnetic and physical properties of  $\text{HoBaCo}_2\text{O}_5$  and another member of the series ( $\text{TbBaCo}_2\text{O}_5$ ) will be published elsewhere.

In the paramagnetic phase,  $T > T_N \sim 340$  K, the crystal structure of  $\text{HoBaCo}_2\text{O}_5$  is tetragonal (space group  $P4/mmm$ ) with cell parameters  $a = b = a_p = 3.891$  Å,  $c = 7.488$  Å  $\sim 2a_p$  (here,  $a_p$  is defined as the pseudocubic cell parameter). The structure derives from the simple perovskite by doubling the cell along the  $c$  axis in order to account for the alternate stacking of oxygen deficient ( $\text{Ho}\square$ ) and oxygen rich ( $\text{BaO}$ ) layers. In  $\text{HoBaCo}_2\text{O}_5$ , the Co ions are enclosed in square base pyramids formed by the five neighboring oxygen ions. When lowering the temperature below  $T_N$ , we observe extra peaks corresponding to the appearance of magnetic moments on the Co ions. These magnetic peaks are indexed with the propagation vector  $\mathbf{k} = (\frac{1}{2}, \frac{1}{2}, 0)$ , meaning that each Co ion is coupled antiferromagnetically (AF) to the six nearest neighbors along the three crystallographic axes (so-called  $G$ -type magnetic structure). Simultaneously to the onset of magnetic ordering, the crystal structure exhibits a

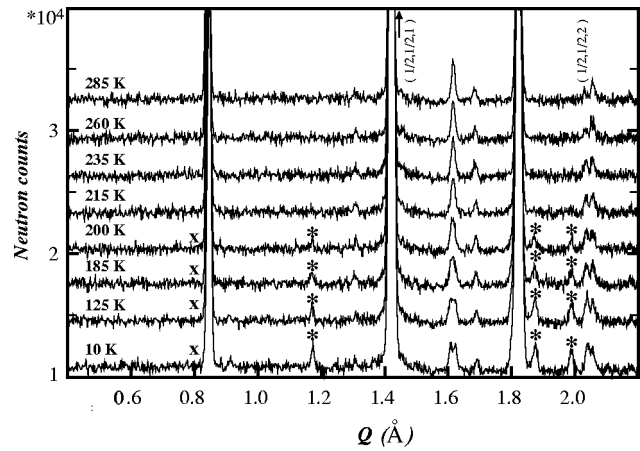


FIG. 2. NPD spectra of  $\text{HoBaCo}_2\text{O}_5$  collected on G6-1. Magnetic peaks are labeled with their indexes referred to the unit cell  $a_p \times a_p \times 2a_p$ . The asterisks indicate superstructure peaks, the x symbol denotes the  $(0, 1/2, 0)$  and  $(1/2, 0, 0)$  forbidden reflections according to the nuclear and magnetic structure, respectively.

small orthorhombic distortion ( $(b-a)/(b+a) \sim 5 \times 10^{-4}$ ). In the new orthorhombic setting (space group  $Pmmm$ ,  $a < b$ ), the Co magnetic moments point along the  $a$  direction. With further cooling, whereas the  $a$  and  $c$  cell parameters decrease continuously, the pseudocubic cell  $b$  parameter increases significantly down to  $T_{CO} \sim 210$  K (Fig. 1). At this temperature, a small discontinuity is observed in the cell volume. As shown in Fig. 2, weak additional reflections are observed below  $T_{CO}$  on the high intensity NPD patterns. These extra reflections account for the doubling of the nuclear unit cell along the  $b$  direction. Note that the crystallographic nature of these superstructure peaks is confirmed by electron diffraction.<sup>14</sup> According to the observed extinction conditions, the new crystal structure is thus described in space group  $Pmmb$  with unit-cell parameters  $a \sim a_p$ ,  $b \sim c \sim 2a_p$ . The main characteristic of this new crystal structure, shown in Fig. 3, is the existence of two independent sites for the cobalt cations, as well as four nonequivalent oxygen atom positions, which could be accurately determined from NPD data refinement. Both Co sites remain enclosed into slightly deformed square base pyramids, but the volumes of these differ considerably, as evidenced by inspection of the

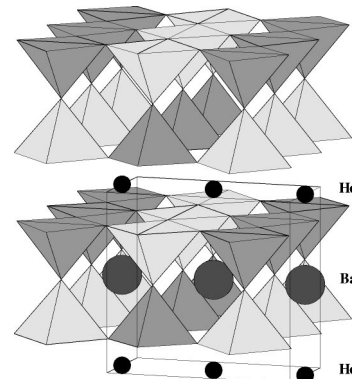


FIG. 3. Crystal structure of  $\text{HoBaCo}_2\text{O}_5$  in the charge ordered phase. The darker and brighter pyramids represent the oxygen environments of  $\text{Co}^{3+}$  and  $\text{Co}^{2+}$  ions, respectively.

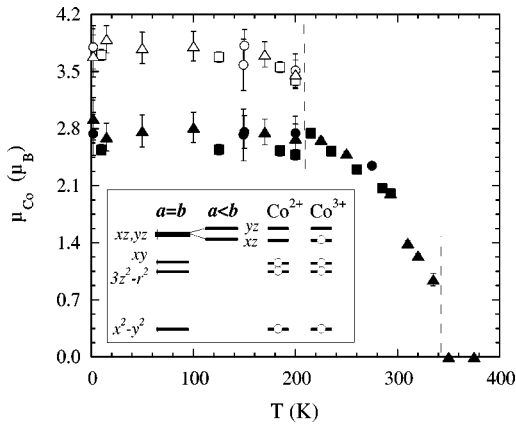


FIG. 4. Temperature dependence of Co magnetic moments in  $\text{HoBaCo}_2\text{O}_5$ . In the inset we have represented the orbital splitting by the pyramidal crystal field and the electronic states of HS- $\text{Co}^{2+}$  and HS- $\text{Co}^{3+}$  (a symbol denotes one hole in the orbital).

Co-O distances. Therefore, from purely steric considerations, we assume each of these sites to be exclusively occupied by  $\text{Co}^{3+}$  or  $\text{Co}^{2+}$  cations. Note that this rather unusual charge ordering leads to the formation of  $\text{Co}^{3+}$  and  $\text{Co}^{2+}$  chains along the  $[100]$  direction and an alternate stacking of these ions along the  $b$  and  $c$  axes. The CO phase is further confirmed by bond valence sum calculations but, to a larger extent, by closer examination of the magnetic structure. In the CO phase, the magnetic moments remain along the  $a$  direction and the saturated values reach  $3.7(2)\mu_B$  and  $2.7(2)\mu_B$  for  $\text{Co}^{3+}$  and  $\text{Co}^{2+}$ , respectively (Fig. 4). Whereas the  $1\mu_B$  difference reflects perfectly the contribution of the additional hole in  $\text{Co}^{3+}$ , the refined moments are in good agreement with the spin-only values expected for high-spin HS- $\text{Co}^{3+}$  and HS- $\text{Co}^{2+}$  ( $4\mu_B$  and  $3\mu_B$ , respectively). Note that the slight reduction from the ideal values can be accounted for within a localized-electron regime by covalency effects. In the Fig. 4 inset, we have represented the crystal-field splitting of the orbital cation  $d$  levels for a square base pyramidal environment.<sup>15</sup> For a slightly orthorhombic distortion of the pyramid ( $a < b$ ), the highest twofold degenerate level is further split, and both  $d_{yz}$  and  $d_{xz}$  orbitals are unoccupied by holes in HS- $\text{Co}^{2+}$ , whereas only the  $d_{yz}$  orbital remains hole free in HS- $\text{Co}^{3+}$ . Within this electronic picture, the  $G$ -type magnetic structure is fully supported by the Goodenough-Kanamori rules for superexchange magnetism.<sup>16,17</sup> Although it is observed in some parent Co based oxides,<sup>7,18</sup> we rule out the possibility of a low-spin or intermediate-spin state for the trivalent cobalt, since these configurations would thus lead to much lower average magnetic moments than those we measured in  $\text{HoBaCo}_2\text{O}_5$ . Finally, we have to point out that, down to the lowest measured temperature (1.5 K), no evidence for long-range ordering of the Ho magnetic moments was detected.

Figure 5 shows the temperature dependence of transport properties measured in  $\text{HoBaCo}_2\text{O}_5$ . The DSC curves exhibits two exothermic (endothermic) peaks around  $T_N$  and  $T_{CO}$  in cooling (heating) runs. These peaks are consistent with the change in entropy caused by the spin and charge ordering at  $T_N$  and  $T_{CO}$ . The 10 K hysteresis between cooling and heating runs suggests a first-order character for these transitions. The temperature dependence of the resistivity clearly indi-

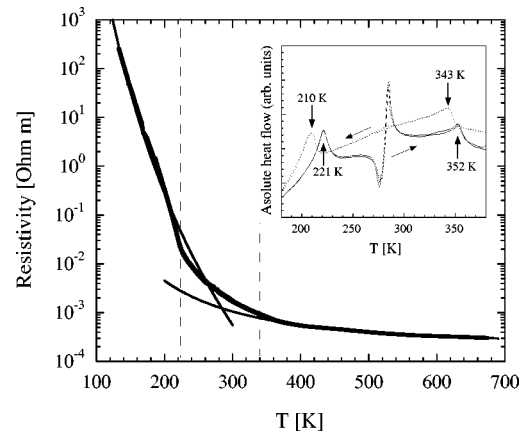


FIG. 5. Resistivity measured in  $\text{HoBaCo}_2\text{O}_5$  and DSC curves obtained on heating and cooling runs (inset). The solid lines show the fit of the resistivity using the models described in the text. On the DSC curves, the ordinate indicates exothermic (endothermic) reaction for heating (cooling) runs. The strong signal on heating runs is due the presence of very small amount of water in the apparatus.

cates an insulating behavior for  $\text{HoBaCo}_2\text{O}_5$  over all the measured temperature range, but with two distinct regimes. Using the general models described by Snyder<sup>19</sup> for insulating oxides, the resistivity is well approximated above  $\sim 360$  K and below  $\sim 210$  K by  $\rho = \rho_0 T \exp(E_A/kT)$  and  $\rho = \rho_0 \exp((T_0/T)^{1/4})$ , respectively. It is very interesting to note the existence of a large intermediate region, which can be described with a combination of the high- and low-temperature models. This region corresponds roughly to the temperature range  $T_{CO} \leq T \leq T_N$  found by NPD. The small discrepancy for the high temperature transition values found by NPD ( $T_N \sim 340$  K) and resistivity (360 K) is explained by short-range magnetic interactions. The increase in resistivity followed by the onset of the AF state would lead us to conclude, similarly to observations made in manganites<sup>9,10</sup> or nickelates,<sup>20</sup> to a preliminary charge ordering at  $T_N$ . However, this effect is not directly observed in our NPD data. It is likely that below  $T_N$  charge localization occurs, but there is a competition between the  $\text{Co}^{2+}$ - $\text{Co}^{2+}$ ,  $\text{Co}^{3+}$ - $\text{Co}^{3+}$ , and  $\text{Co}^{2+}$ - $\text{Co}^{3+}$  couplings along the three crystallographic axes. In the latter coupling, the  $d_{xz}$  electron is not completely localized on one of the cobalt ions and so conduction over Co-Co distance ranges remain possible. Nevertheless, due to the small extent of  $d_{xz}$  orbitals, this conduction effect remains rather small. Below  $T_{CO}$ , the  $d_{xz}$  electrons are well localized on the Co site, leading to the CO phase described in this letter, and  $\text{HoBaCo}_2\text{O}_5$  becomes highly insulating.

In conclusion, we have observed in  $\text{HoBaCo}_2\text{O}_5$  a well established CO phase associated with a change in the conductivity and occurring at a temperature much lower than the onset of AF ordering. According to our NPD data, no indication of a long-range charge ordering could be detected in the intermediate temperature range  $T_{CO} \leq T \leq T_N$ . This is true even if the AF spin ordering is correlated with a reduction in the conductivity. Further experiments could eventually support an incomplete or short-range charge ordering occurring at  $T_N$ . The complete charge-ordered state appears at a lower temperature,  $T_{CO} \sim 210$  K, and is responsible for a

structural transition. The  $1\mu_B$  difference between the two independent Co sites corroborates our CO picture. These results are of prime importance for understanding charge localization effects. A last interesting point concerns the interactions responsible for the *G*-type structure. Although the Co-Co interactions through the oxygen atoms are well explained within the superexchange framework, there is still an ambiguity about the  $\text{Co}^{2+}$ - $\text{Co}^{3+}$  coupling through the vacant site of the Ho□ layer. Direct exchange only, expected to

lead to a ferromagnetic coupling, appears improbable from the small orbital overlap. Therefore superexchange-type mechanisms involving different paths may be postulated. Such questions could be well answered from a complete study of the  $L_n\text{BaCo}_2\text{O}_{5+\delta}$  ( $0 \leq \delta \leq 1$ ) systems, for which there are oxygen ions available for cobalt superexchange coupling through the Ho□ layer.

The authors thank Dr. M. T. Fernández-Díaz for fruitful discussions.

- 
- <sup>1</sup>R. Mahendiran, A. K. Raychaudhuri, A. Chainani, and D. D. Sarma, *J. Phys. C* **10**, L562 (1995).  
<sup>2</sup>C. Martin, A. Maignan, D. Pelloquin, N. Nguyen, and B. Raveau, *Appl. Phys. Lett.* **71**, 1421 (1997).  
<sup>3</sup>Y. Moritomo, M. Takeo, X. J. Liu, T. Akimoto, and A. Nakamura, *Phys. Rev. B* **58**, R13 334 (1998).  
<sup>4</sup>I. O. Troyanchuk, N. V. Kasper, D. D. Khalyavin, A. N. Chobot, G. M. Chobot, and H. Szymczak, *J. Phys. C* **10**, 6381 (1998).  
<sup>5</sup>A. Maignan, C. Martin, D. Pelloquin, N. Nguyen, and B. Raveau, *J. Solid State Chem.* **142**, 247 (1999).  
<sup>6</sup>D. Akahoshi and Y. Ueda, *J. Phys. Soc. Jpn.* **68**, 736 (1999).  
<sup>7</sup>E. Suard, F. Fauth, and V. Caignaert, *Physica B* **276–278**, 254 (2000).  
<sup>8</sup>W. Zhou, C. T. Lin, and W. Y. Liang, *Adv. Mater.* **5**, 735 (1993).  
<sup>9</sup>N. Kumar and C. N. R. Rao, *J. Solid State Chem.* **129**, 363 (1997); A. Arulraj, P. N. Santhosh, R. Srinivasa Gopalan, A. Guha, A. K. Raychaudhuri, N. Kumar, and C. N. R. Rao, *J. Phys.: Condens. Matter* **10**, 8497 (1998).  
<sup>10</sup>P. G. Radaelli, D. E. Cox, M. Marezio, and S. W. Cheong, *Phys. Rev. B* **55**, 3015 (1997).  
<sup>11</sup>C. H. Chen and S. W. Cheong, *Phys. Rev. Lett.* **76**, 4042 (1996).  
<sup>12</sup>F. Millange, V. Caignaert, B. Domengès, and B. Raveau, *Chem. Mater.* **10**, 1974 (1998).  
<sup>13</sup>J. Rodriguez-Carvajal, *Physica B* **192**, 55 (1993).  
<sup>14</sup>B. Domengès and V. Caignaert (private communication).  
<sup>15</sup>J. J. Zuckermann, *J. Chem. Educ.* **42**, 135 (1965).  
<sup>16</sup>J. B. Goodenough, *Phys. Rev.* **100**, 564 (1955).  
<sup>17</sup>J. Kanamori, *J. Phys. Chem. Solids* **10**, 87 (1959).  
<sup>18</sup>D. Bahadur, S. Kollali, C. N. R. Rao, M. J. Patni, and C. M. Srivastava, *J. Phys. Chem. Solids* **40**, 981 (1979).  
<sup>19</sup>G. J. Snyder, C. H. Booth, F. Bridges, R. Hiskes, S. DiCarolis, M. R. Beasley, and T. H. Geballe, *Phys. Rev. B* **55**, 6453 (1997).  
<sup>20</sup>J. A. Alonso, J. L. García-Munoz, M. T. Fernández-Díaz, M. A. G. Aranda, M. J. Martínez-Lope, and M. T. Casais, *Phys. Rev. Lett.* **82**, 3871 (1999).